Previews

Regulation of product distribution in CO_2 hydrogenation to light olefins

Wenna Zhang[1] and Yingxu Wei[1,*]

Conversion of CO_2 into specific light olefins with high selectivity is a challenge. In this issue of *Chem*, Fan and co-workers propose an ethanol-intermediate route with the design of a new catalyst: Cr_2O_3(SG)/H-SAPO-34. The $C_2^=–C_4^=$ selectivity can reach 95.7%, and ethene accounts for 74% of light olefins in CO_2 hydrogenation.

The massive emission of carbon dioxide (CO_2) leads to a serious greenhouse effect, which is a major constraint on economic and social development. On the other hand, CO_2 is also a clean, non-toxic, and abundant carbon-containing resource. Using CO_2 as a raw material can not only reduce the amount of CO_2 in the atmosphere and slow down the greenhouse effect but also open up a new way to prepare clean fuels. CO_2 can be catalyzed into a variety of chemicals, among which light olefins are important building blocks in modern chemical industry.[1]

Nowadays, direct hydrogenation of CO_2 into light olefins can be achieved by Fischer-Tropsch (FT) synthesis and methanol-intermediate routes. In FT synthesis, CO_2 is generally transformed into CO via the reverse water-gas shift (RWGS) reaction and then into light olefins via the coupling of CH_x intermediates.[2] Because the distribution of hydrocarbon products follows the ASF rule, the light-olefin selectivity in FT synthesis is no higher than 61%, whereas that of methane reaches 15%–25%. The recently proposed methanol-intermediate route gave a different manner for light-olefin formation in CO/CO_2 hydrogenation. Methanol intermediate is generated on metal oxides and rapidly diffuses onto the acid sites of zeolite to produce light olefins via dehydration and C–C coupling.[3,4] Compared with the FT synthesis route,

the methanol-intermediate route can effectively break the limitation of the ASF rule and increase the selectivity of light olefins in hydrocarbons to 70%–87%.[5] Nevertheless, further elevation of light-olefin selectivity beyond 90% is still quite difficult. Moreover, the composition of light olefins is rather fixed at ~25%–30% ethene, ~35%–40% propene, and ~10%–15% butene. Although some research has indicated that a change in zeolite structure and acidic properties can modulate the distribution of light olefins,[6,7] the highly selective generation of a single specific olefin remains a challenge.

In this issue of *Chem*, Fan and co-workers propose the new concept of an ethanol-intermediate route for direct conversion of CO_2 into light olefins abundant in ethene.[8] They first fabricated a composite catalyst consisting of Cr_2O_3 prepared by the sol-gel method and H-SAPO-34 zeolite prepared by the hydrothermal synthesis method. *In situ* X-ray diffraction, *in situ* X-ray photoelectron spectroscopy, transmission electron microscopy (TEM), high-resolution TEM, and selected-area electron diffraction results indicated that Cr_2O_3(SG) oxide has a hexagonal structure with uniform dispersion of Cr and O atoms. Pre-treatment with hydrogen (H_2) resulted in the reduction of Cr^{6+} to Cr^{3+} and the formation of more surface oxygen vacancies benefitting the adsorption and activation of CO_2. H-SAPO-34 showed a cubic morphology with high crystallinity.

Powder mixing of Cr_2O_3(SG) oxide and H-SAPO-34 zeolite did not significantly affect their crystal structure.

In CO_2 hydrogenation, the Cr_2O_3(SG)/H-SAPO-34 bifunctional catalyst gave a $C_2^=–C_4^=$ selectivity in hydrocarbons and an olefin-to-paraffin (O/P) ratio as high as 95.8% and 41.5, respectively, at 370°C and 0.5 MPa (Figure 1A). Of note, the ethene selectivity accounted for ~70% of the light olefins with an ethene-to-propene (E/P) ratio higher than 2.6. These results are superior to those on $ZnZrO_x$/H-SAPO-34, $ZnAl_2O_4$/H-SAPO-34, $ZnGa_2O_4$/HSAPO-34, $InZrO_x$/H-SAPO-34, and $ZnCrO_x$/H-SAPO-34 in CO_2 hydrogenation under the same conditions (Figure 1B).

The authors further investigated the influence of reaction temperature, pressure, space velocity, the synthesis method of metal oxide, and the integration manner between metal oxide and zeolite on the catalytic activity and product distribution. Cr_2O_3(SG)/H-SAPO-34 also exhibited good catalytic stability and regenerability. After 600 h of reaction, the selectivity of ethene and $C_2^=–C_4^=$ in hydrocarbons could be maintained at 62.5% and 91.0%, respectively. The used catalyst was subsequently regenerated by H_2 or 2% O_2/Ar at 500°C–550°C. After ten recycles (above 1,000 h), it still gave ethene and $C_2^=–C_4^=$ selectivities of 61% and 92%, respectively, with an E/P ratio of 2.3.

The catalytic performance of pure Cr_2O_3(SG) in CO_2 hydrogenation was then evaluated, and some ethanol (in addition to methanol) was detected at the initial reaction stage. This implies

[1]National Engineering Laboratory for Methanol to Olefins, Dalian National Laboratory for Clean Energy, iChEM (Collaborative Innovation Center of Chemistry for Energy Materials), Dalian Institute of Chemical Physics, Chinese Academy of Sciences, Dalian 116023, P.R. China
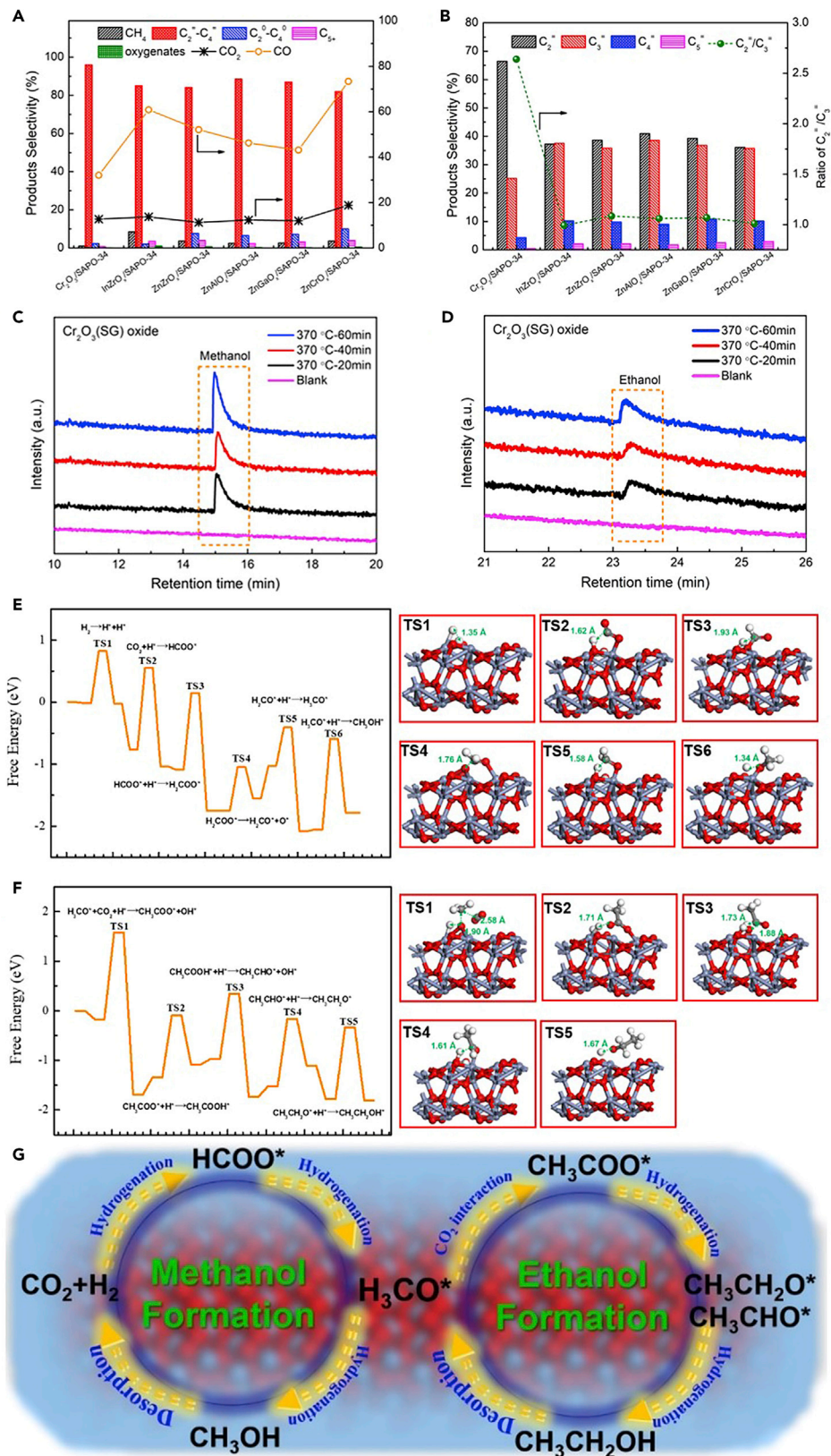
*Correspondence: weiyx@dicp.ac.cn

Figure 1. CO$_2$ hydrogenation to light olefins on Cr$_2$O$_3$(SG)/H-SAPO-34

(A and B) CO$_2$ conversion and product selectivity (A) and olefin selectivity and E/P ratio (B) on various metal oxide/H-SAPO-34 bifunctional catalysts. Reaction conditions: H$_2$/CO$_2$ = 3:1, GHSV = 4,000 mL g^{-1} h^{-1}, 0.5 MPa, and 370°C.

(C and D) GC-MS diagrams of the methanol (C) and ethanol (D) in effluents obtained at different reaction times on Cr$_2$O$_3$(SG). Reaction conditions: H$_2$/CO$_2$ = 3:1, 0.5 MPa, and 370°C.

(E and F) Free-energy profiles and the optimized transition states for CO$_2$ hydrogenation to methanol (E) and ethanol (F) on Cr$_2$O$_3$.

(G) Reaction scheme for CO$_2$ hydrogenation to methanol and ethanol on Cr$_2$O$_3$.

Adapted from Fan and co-workers.[8]

that the high ethene selectivity of Cr$_2$O$_3$(SG)/H-SAPO-34 in CO$_2$ hydrogenation could originate from the rapid conversion of generated ethanol and methanol intermediates on Cr$_2$O$_3$ to ethene and light olefins on the acid sites of H-SAPO-34. It was verified that feeding a methanol-ethanol mixture on H-SAPO-34 can significantly improve the ethene selectivity, whereas for the typical methanol conversion process, the ethene selectivity is no higher than 40%, as previously reported.[9]

The authors systemically investigated the reaction mechanism for CO$_2$ activation and the formation and evolution of various intermediates (including formate, methoxy, acetate and ethoxy species) by combining *in situ* diffuse reflectance infrared Fourier transform spectroscopy (DRIFTS), isotope-labeled *in situ* DRIFTS, gas chromatography-mass spectrometry (GC-MS), and theoretical calculation. In CO$_2$ hydrogenation on Cr$_2$O$_3$(SG), the characteristic peaks of formate at 1,592, 1,562, 1,354, and 1,307 cm^{-1} and of methoxy at 1,025–1,090 cm^{-1} were clearly identified, and their intensities gradually increased with the reaction time. In addition, the bands ascribed to acetate (1,541 and 1,620 cm^{-1}), acetaldehyde (1,575 and 1,715 cm^{-1}), and ethoxy (1,012 cm^{-1}) were visible at the initial stage. In the effluents, some ethanol was detectable even though their amounts were much lower than that of methanol (Figures 1C and 1D).

As a comparison, only the signal peaks of formate and methoxy species were observed in the *in situ* DRIFTS of ZnZrO$_x$ in CO$_2$ hydrogenation, and no ethanol could be detected in the effluents. Therefore, upon coupling with

H-SAPO-34, ZnZrO$_x$/H-SAPO-34 exhibited an ethene selectivity of only 38.6%, such that the light-olefin distribution was similar to the typical methanol-to-olefin process.

The reaction kinetics of various elemental steps for methanol and ethanol formation were investigated by density functional theory (DFT) calculation and molecular dynamics (MD) simulation. The CO$_2$ hydrogenation to HCOO*, H$_3$CO*, and CH$_3$OH* needs to overcome free-energy barriers of 0.62–1.45 eV (Figure 1E). The reaction of H$_3$CO* with CO$_2$ and H* to form CH$_3$COO* and OH* requires a higher free-energy barrier of 1.74 eV even though hydrogenation of CH$_3$COO* to CH$_3$CH$_2$OH* requires lower free-energy barriers of 1.25–1.44 eV (Figure 1F). This result indicates that methanol formation is easier than ethanol on Cr$_2$O$_3$.

It is worth noting that introducing CO into the feedstocks leads to the formation of more methane and C$_2^0$–C$_4^0$ at the expense of ethene and light olefins. This is because CO can be directly dissociated and hydrogenated to form alkanes on Cr$_2$O$_3$. Indeed, DFT calculation suggests that the free-energy barrier of the rate-determining step for methane formation via CO dissociation and hydrogenation is comparable to that of methanol and ethanol formation. Therefore, the intensity of peaks characteristic of formate, acetate, methoxy, and ethoxy in the *in situ* DRIFTS is much weaker in CO hydrogenation than in CO$_2$ hydrogenation.

In summary, effectively regulating the light-olefin distribution and selectively promoting the formation of a single specific olefin are highly desirable. In this

issue of *Chem*, Fan and co-workers propose a new strategy to improve ethene selectivity by forming an ethanol intermediate on Cr$_2$O$_3$(SG) oxides and then rapidly converting the generated ethanol into ethene on H-SAPO-34 (Figure 1G). The prepared Cr$_2$O$_3$(SG)/H-SAPO-34 composite catalyst shows high ethene and light-olefin selectivity in CO$_2$ hydrogenation, and no significant deactivation was observed even after 600 h of reaction. The results of *in situ* spectroscopy, DFT calculation, and MD simulation indicate that ethanol is generated from the hydrogenation of CH$_3$COO* intermediate, which is formed through the reaction of H$_3$CO* with CO$_2$ and H*.

DECLARATION OF INTERESTS

The authors declare no competing interests.

1. Centi, G., Quadrelli, E.A., and Perathoner, S. (2013). Catalysis for CO$_2$ conversion: A key technology for rapid introduction of renewable energy in the value chain of chemical industries. Energy Environ. Sci. 6, 1711–1731. https://doi.org/10.1039/c3ee00056g.

2. Torres Galvis, H.M., and de Jong, K.P. (2013). Catalysts for production of lower olefins from synthesis gas: A review. ACS Catal. 3, 2130–2149. https://doi.org/10.1021/cs4003436.

3. Jiao, F., Li, J.J., Pan, X.L., Xiao, J.P., Li, H.B., Ma, H., Wei, M.M., Pan, Y., Zhou, Z.Y., Li, M.R., et al. (2016). Selective conversion of syngas to light olefins. Science 351, 1065–1068. https://doi.org/10.1126/science.aaf1835.

4. Cheng, K., Gu, B., Liu, X.L., Kang, J.C., Zhang, Q.H., and Wang, Y. (2016). Direct and highly selective conversion of synthesis gas into lower olefins: Design of a bifunctional catalyst combining methanol synthesis and

carbon-carbon coupling. Angew. Chem. Int. Ed. *55*, 4725–4728. https://doi.org/10.1002/anie.201601208.

5. Bao, J., Yang, G.H., Yoneyama, Y., and Tsubaki, N. (2019). Significant advances in C1 catalysis: Highly efficient catalysts and catalytic reactions. ACS Catal. *9*, 3026–3053. https://doi.org/10.1021/acscatal.8b03924.

6. Wang, M.H., Kang, J.C., Xiong, X.W., Zhang, F.Y., Cheng, K., Zhang, Q.H., and Wang, Y. (2021). Effect of zeolite topology on the hydrocarbon distribution over

bifunctional ZnAlO/SAPO catalysts in syngas conversion. Catal. Today *371*, 85–92. https://doi.org/10.1016/j.cattod.2020.07.076.

7. Wang, S., Zhang, L., Zhang, W.Y., Wang, P.F., Qin, Z.F., Yan, W.J., Dong, M., Li, J.F., Wang, J.G., He, L., et al. (2020). Selective conversion of CO2 into propene and butene. Chem *6*, 3344–3363. https://doi.org/10.1016/j.chempr.2020.09.025.

8. Wang, S., Zhang, L., Wang, P., Liu, X., Chen, Y., Qin, Z., Dong, M., Wang, J., He, L., Olsbye, U.,

and Fan, W. (2022). Highly effective conversion of CO2 into light olefins abundant in ethene. Chem *8*, 1376–1394. https://doi.org/10.1016/j.chempr.2022.01.004.

9. Hereijgers, B.P.C., Bleken, F., Nilsen, M.H., Svelle, S., Lillerud, K.P., Bjørgen, M., Weckhuysen, B.M., and Olsbye, U. (2009). Product shape selectivity dominates the methanol-to-olefins (MTO) reaction over HSAPO-34 catalysts. J. Catal. *264*, 77–87. https://doi.org/10.1016/j.jcat.2009.03.009.

Operando scattering techniques for detecting precipitation reactions in lithium-sulfur batteries

Qining Fan[1] and Jiazhao Wang[1,*]

Precipitation behavior is crucial to utilizing sulfur cathodes in lithium-sulfur (Li-S) batteries. In this issue of *Chem*, Rennie and co-workers apply *operando* scattering techniques to reveal correlations between precipitation reactions and the electrochemical performance of sulfur cathodes and demonstrate that Li$^+$ supply in carbon mesopores is significant for precipitation reactions and thus sulfur utilization.

The demand for batteries with high energy density, good longevity, low cost, and high safety is impelling academics and industry to develop new battery systems to replace the state-of-the-art lithium (Li)-ion batteries. Rechargeable lithium-sulfur (Li-S) batteries are very promising for such next-generation batteries because they can theoretically deliver high energy density (~2,600 Wh kg^{-1}) and because S is cheap and environmentally friendly.[1] However, practical application is the "holy grail" of Li-S batteries because of the challenges with Li anodes, electrolytes, and S cathodes. In particular, on the S cathode side, the non-conductive solid S and Li$_2$S (discharge product) lead to the low utilization of S cathodes and generally reduce the energy density of Li-S batteries to <300 Wh kg^{-1}.[2]

S cathodes experience an electrochemical conversion between S and Li$_2$S. In the last two decades, most research on S cathodes has focused on the activation of non-conductive solid S$_8$, and sophisticated cathode preparation methods and various conductive materials have shown their effectiveness in enhancing charge transfer to and from the non-conductive S$_8$ to improve the utilization of S cathodes,[3] although the problem of the non-conductive solid discharge product Li$_2$S has always been overlooked. This problem should receive more attention because S can be regulated during the electrode preparation, but the Li$_2$S distribution and precipitation rely on the electrode composition and structure in the electrochemical environment and significantly influence the electrochemical

performance of S cathodes in terms of capacity, voltage plateau, and rate performance.[4,5]

The precipitation of Li$_2$S from soluble long-chain lithium polysulfide (Li$_2$S$_{4–8}$) intermediates seems inevitable, especially in the ether-based electrolytes generally used in Li-S batteries, because the dissolution of Li$_2$S$_{4–8}$ plays a crucial role in the initial stage of S$_8$ conversion to Li$_2$S$_{4–8}$.[6] The research on Li$_2$S precipitation on elaborately designed open carbon materials with excess electrolyte has demonstrated the importance of high surface areas of carbon materials in accelerating Li$_2$S precipitation and enabling high S utilization.[7] Nevertheless, in a practical S cathode, the carbon materials are porous, and the electrolyte in the pores is limited, leading to high complexity in Li$_2$S precipitation. Although the pores of carbon materials can provide a large surface area, the concentration of non-conductive Li$_2$S precipitates on the S cathode by uncontrolled Li$_2$S precipitation can block most porous structures, causing sluggish Li-ion transfer throughout the whole cathode, increased polarization, and low capacity.[4] Therefore, discrepancies between

[1]Institute for Superconducting & Electronic Materials, Australian Institute of Innovative Materials, University of Wollongong, NSW 2522, Australia

*Correspondence: jiazhao@uow.edu.au